

*International Journal of*

# Oil, Gas and Coal Technology



---

## Pore structure and its impact on CH<sub>4</sub> adsorption capability and diffusion characteristics of normal and deformed coals from Qinshui Basin

---

Shou-qing Lu, Yuan-ping Cheng\*

National Engineering Research Center of Coal Gas Control,  
China University of Mining & Technology,  
Xuzhou, Jiangsu 221116, China  
Email: lushouqing2006@163.com  
Email: yuanpingcheng@yahoo.cn  
Email: ypchengcumt@hotmail.com  
\*Corresponding author

Wei Li

Faculty of Safety Engineering,  
China University of Mining & Technology,  
Xuzhou, Jiangsu 221116, China  
Email: liwei5005@126.com

Liang Wang

Key Laboratory of Gas and Fire Control for Coal Mine,  
China University of Mining & Technology,  
Xuzhou, Jiangsu 221116, China  
Email: liangw1982@126.com

**Abstract:** In this study, the pore structure, adsorption/desorption kinetics and thermodynamics of normal and deformed coals are compared. The total pore volume and porosity of deformed coal are 2.84 to 2.91 times greater than those of normal coal, whereas the micropore volume and specific surface area of normal coal are 1.15 to 1.35 times greater than those of deformed coal. Langmuir volume of normal coal is greater than that of deformed coal.  $\Delta\sigma$  of normal coal is slightly greater than that of deformed coal which indicates that the unit area of normal coal CH<sub>4</sub> adsorption capacity is also greater than that of deformed coal. At the early stage of the desorption process, the mass diffusivity of deformed coal is ten times greater than that of normal coal. Then it decreases rapidly, while that of normal coal decreases very slowly. At last, it will be less than that of normal coal.

**Keywords:** normal coal; deformed coal; pore structure; surface free energy; mass diffusivity;

**Reference** to this paper should be made as follows: Lu, S., Cheng, Y., Li, W. and Wang, L. (2015) 'Pore structure and its impact on CH<sub>4</sub> adsorption capability and diffusion characteristics of normal and deformed coals from Qinshui Basin', *Int. J. Oil, Gas and Coal Technology*, Vol. 10, No. 1, pp.94–114.

**Biographical notes:** Shou-qing Lu is a member of National Engineering Research Center of Coal Gas Control at Xuzhou. He received his BSc in Safety Engineering and MSc in Safety Technology and Engineering from China University of Mining & Technology. His current research interests are in coal mine gas prevention and control, coal and gas outburst and the theory, and technology of pressure relief gas drainage.

Yuan-ping Cheng is a Professor of China University of Mining & Technology, the Director of National Engineering Research Center of Coal Gas Control at Xuzhou and expert of national work safety experts panel. He received his BSc from Liaoning Technical University in 1984, and MSc (1987) and PhD (1990) from China University of Mining & Technology. He is an Associate Editor-in-Chief of *Journal of Coal Science & Engineering* and an Editor of *Mining Science and Technology*. His research interests include coal mine gas prevention and control and building fire protection theory and engineering application. He has been a consultant and lecturer to several organisations and mining corporations. For his research and educational achievements, he has received numerous recognitions and awards.

Wei Li is a Lecturer at China University of Mining & Technology at Xuzhou. He received his BSc in Safety Engineering from Zhongyuan University of Technology and PhD in Safety Technology and Engineering from China University of Mining & Technology. His research is focused on the mechanism of CO<sub>2</sub> pools formation, CO<sub>2</sub> control technology and the theory and technology of pressure relief CO<sub>2</sub> drainage.

Liang Wang is an Associate Professor at China University of Mining & Technology at Xuzhou. He received his PhD in Safety Technology and Engineering from China University of Mining & Technology. He is an Editor of *Journal of Coal Science & Engineering*. His research interests are in the fields of prevention measures for gas disasters, the theory and technology of pressure relief gas drainage, and fracture evolution of distant pressure relief coal-rock masses.

---

## 1 Introduction

China lacks oil and natural gas, and coal provides more than 70% of the country's energy (Cattaneo et al., 2011). Coal and gas outbursts in Chinese coal mines are very serious safety hazards. By October 2010, 647 coal and gas outbursts had occurred in China's mines (Yang et al., 2012a). With a mining depth speed of 10 to 20 metre per year in deep areas, the number of coal and gas outbursts in coal mines will continue to increase. However, because China's economy continues to develop at a rapid pace, dangerous coal and gas outbursts are likely to continue for years to come (Yang et al., 2012b).

Coal is a special type of rock with low strength and a high Poisson's ratio and is uniquely sensitive to stress and strain. Deformed coal can record the effect of tectonic stress in stratum (Jiang et al., 2010; Li et al., 2011). Deformed coal is coal that experiences plastic, ductile and flowing deformation due to repeated tectonic activity over long periods of time. The thickening of deformed coal zones increases the capacity for methane storage, and compressed structures within deformed coal zones may act as tectonic screens, blocking methane migration, which can result in high-pressure pockets

of methane pressure (Li, 2001). Thus, a thick zone of deformed coal provides conditions favourable to coal and gas outbursts. Cao et al. (2003) found that most coal and gas outbursts in the Pingdingshan coalfield occurred in areas where the thickness of the deformed coal zone had increased.

In most cases, a single coal seam often contains several normal and deformed coal sub-layers. These sub-layers are usually very different from each other, especially in their pore structure, adsorption capability and diffusion characteristics, as shown by many researchers (Yang et al., 2012a). Mercury porosimetry and N<sub>2</sub> adsorption are used to characterise the tectonism-influenced range of pore structures. Some researchers (Wang and Yang, 1980; Hower, 1997) find that tectonism increases the pores with diameters from 2 nm to 7500 nm and micropores with diameters less than 2 nm are not affected, however, Ju and Li (2009) find that tectonism may destroy micropores with diameters less than 2.5 nm. Micropores play a major role in the total specific surface area and adsorption capacity of coal (Clarkson and Bustin, 1999). Wang and Yang (1980) think that the adsorption capability difference between normal coal and deformed coal is not obvious. What's more, Yao and Lv (1996) suggest that the adsorption capacity of deformed coal is larger than that of normal coal at a low adsorption pressure, and there is no difference on the adsorption capacity at high adsorption pressure. In addition, Cao et al. (2003) considers that deformed coal has a higher adsorption capacity because deformed coal has a smaller particle size distribution and greater surface areas compared to the normal coal. The desorption velocity of deformed coal is higher than that of normal coal (Wen et al., 2011). At the initial times, the mass diffusivity of the deformed coal is also higher than that of normal coal in condition that the calculation of the mass diffusivity is not dependent on time (Zhang, 2011). However, if the mass diffusivity depends on time, it is necessary to determine whether the mass diffusivity of deformed coal is always higher than that of normal coal.

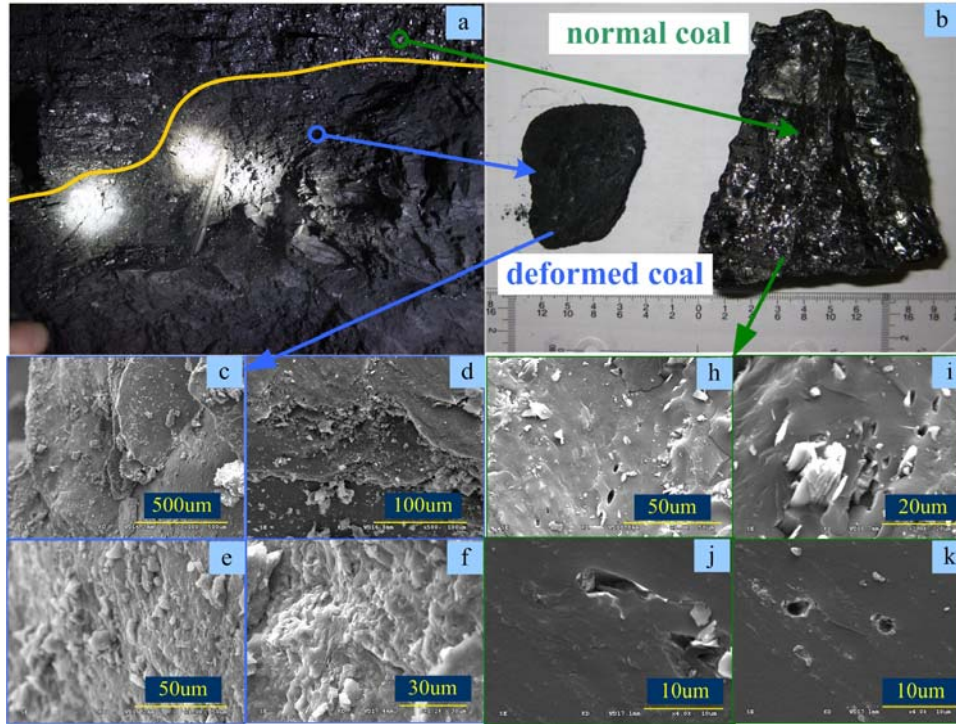
The Daning coal mine is located at the southeastern edge of the Qinshui Basin in Shangxi Province in China. The No. 3 coal seam is the primary coal bed of the Daning coal mine and is suitable for mining, despite the hazards of coal and gas outbursts. Since the Indosinian period, the southeastern edge of the Qinshui Basin has been enriched by repeated and long-term tectonic action. The thickness of the No. 3 coal seam is 4.5 m. The lower part of the No. 3 coal seam is a deformed sub-layer with a thickness of 0.5–1.5 m, and the upper part is a normal sub-layer. In this study, the pore structure, adsorption/desorption kinetics and adsorption thermodynamics of normal coal and deformed coal were compared to promote further understanding of the pore structure and its impact on CH<sub>4</sub> adsorption capability and diffusion characteristics.

## **2 Materials and methods**

### *2.1 Origin and characteristics of coal samples*

During this investigation, four coal samples from two locations were obtained, the samples of the normal and deformed coals were selected from different sub-layers at the same location. #1 and #2 are the coal samples from the normal sub-layer and the deformed sub-layer at one location, respectively. 3# and 4# are the coal samples from the normal sub-layer and the deformed sub-layer at another location, respectively.

**Figure 1** (a) Sampling locations (b) normal coal and deformed coal samples (c) SEM photograph of deformed coal samples,  $\times 100$  (d) SEM photograph of deformed coal samples,  $\times 500$  (e) SEM photograph of deformed coal samples,  $\times 1000$  (f) SEM photograph of deformed coal samples,  $\times 1200$  (h) SEM photograph of normal coal samples,  $\times 1000$  (i) SEM photograph of normal coal samples,  $\times 2000$  (j) SEM photograph of normal coal samples,  $\times 4000$  (k) SEM photograph of normal coal samples,  $\times 4000$  (see online version for colours)



After sampling, the coal samples were selected and crushed into different sizes for different tests. The coal samples were experimented as a single test, and the analyses on coal were made based on the two locations' samples. Scanning electron microscopy (SEM) was conducted (HITACHI S-3000N, Japan) using experimental coal samples formed into approximate cubes with dimensions of 10 mm  $\times$  10 mm  $\times$  10 mm. The distributions of the normal and deformed sub-layers and the SEM results are shown in Figure 1. The normal coal's lustre is bright, while the deformed coal's colour is muted. There is an irregular layered structure [Figure 1(c), Figure 1(d)] and a mixed crushing section [Figure 1(e), Figure 1(f)], which were caused by tectonism. There are almond-shaped pores [Figure 1(h)], burst-like pores [Figure 1(i), Figure 1(j)] and rounded pores [Figure 1(k)] in the normal coal.

Proximate analysis was conducted in accordance with the American Society for Testing and Materials (ASTM) standard (ASTM, 2007) using 5E-MAG6600 equipment made in China. The maceral composition of the coals was determined by incident light microscopy and oil immersion in accordance with international standards (Taylor et al., 1998). Maximum vitrinite reflectance ( $R_{o, \max}$ ) measurements were performed using a German-made Zeiss microscope photometer in accordance with international standards (BS ISO 7404-5, 2009). The firmness coefficient was measured using the method

described by Cao et al. (2003). The key parameters of the coal samples are shown in Table 1. Compared with normal coal, the mineral content of the deformed coal is much greater, whereas the firmness coefficient is lower. The moisture, ash, and  $R_{o, \max}$  values of the deformed coal are slightly higher than those of the normal coal.

**Table 1** Key parameters of selected coal samples

Sample no.	Proximate analysis (wt.%)			Macerals (vol.%)			$R_{o, \max}$ (%)	$f$
	Moist	Ash	VM	V	I	M		
#1	1.46	18.14	12.29	75.79	21.87	2.44	3.16	2.00
#2	1.55	22.15	11.01	84.35	6.63	6.02	3.29	0.33
#3	3.28	21.14	8.01	82.80	14.29	2.91	2.73	1.71
#4	3.56	22.41	10.22	75.89	13.85	10.26	2.76	0.25

Notes: Moist = moisture; ash is on a dry basis; VM = volatile matter, on a dry ash-free (daf) basis; V = vitrinite, I = inertinite, M = mineral;  $R_{o, \max}$  = maximum vitrinite reflectance (% oil); and  $f$  = firmness coefficient.

Mercury porosimetry was conducted in accordance with international standards (BS ISO 15901-1, 2005) using the Auto Pore IV 9510 device made in the USA using block-shaped coal samples of 30 to 50 mm on a side. In this study, mercury porosimetry was used to measure pore with diameters as small as 3 nm. The pore size and pore structure can be determined by analysing the intrusion and extrusion curves obtained from mercury porosimetry (Amarasekera et al., 1975). This relationship of mercury intrusion pressure and pore diameter can be obtained by the Young-Laplace law for the particular case of cylindrical pores which can be justified by the curves of mercury injection and withdrawal (Amarasekera et al., 1975) as the Washburn equation, and it is shown in equation (1).

$$d_i = \frac{-4\gamma \cos \theta}{p_i} \quad (1)$$

The volumes, surface areas, and size distributions of the micropores were determined using low-pressure  $\text{CO}_2$  at 273 K (AUTOSORB-1, USA) in accordance with international standards (BS ISO 15901-3, 2007). For the  $\text{CH}_4$  adsorption isotherm, crushed coal samples weighing 50 g and 0.2 to 0.25 mm in particle size were exposed to gas pressures up to 5 MPa at 303 K, 313 K, 323 K, 333 K. The sorption isotherms were determined using the manometric method described by Busch et al. (2004).

For the  $\text{CH}_4$  diffusion experiment, crushed coal samples with 50 g and 1- to 3-mm particle size were used. The experimental coal samples were first placed into the sample cell, which was connected to a vacuum pump at a pressure of  $-13$  KPa for 24 hours. Second, 99.9%  $\text{CH}_4$  gas was injected into the sample cell, which was placed in a water bath at a temperature of 303 K until it reached the desired high pressure (0.8 MPa or 2.4 MPa). The cell was held at a constant  $\text{CH}_4$  pressure for a few days to allow  $\text{CH}_4$  diffusion into the coal and to reach sorption equilibrium. Sudden decompression was then achieved by opening the valve to permit exchange with the atmosphere. During this time, the sample cell was connected to a measuring cylinder for 120 min.

## 2.2 Adsorption kinetics model and thermodynamic theory

### 2.2.1 Adsorption kinetics model

There are many theoretical isothermal sorption models for describing the sorption behaviour of coal. Among these are the Langmuir monolayer sorption model, the BET multilayer sorption model and the Polyanyi sorption potential theory model (the Dubinin-Astakhov equation). Langmuir model is very well suited for describing type I adsorption isotherm, applying to activated carbon or the uniform surface of the solid. What's more, BET multilayer sorption model is suited for describing type I, II or III adsorption isotherm, and it is more for the porous material with abundant mesopores and relative pressure about 0.35~0.7 of multi-molecular of physical adsorption. Polyanyi sorption potential theory model is more used in the capillary condensation phenomenon of smaller pore diameter of adsorbent (Clarkson et al., 1997). The Langmuir model is not suited for high pressure ( $P > 8\sim 10$  MPa) gas adsorption, multi-molecular layer adsorption and heterogeneous surface adsorption, however, it is widely used to study the adsorption characteristics of coal because of its concise form. The Langmuir model is based on the concept of dynamic equilibrium between the rates of sorption of gas on a solid and desorption from the solid surface (Langmuir, 1918). The equation for the Langmuir isotherm is given as follows:

$$V = \frac{abP}{1 + bP} = \frac{V_L P}{P_L + P} \quad (2)$$

According to the monolayer sorption assumption, the specific surface area of coal can be expressed as follows:

$$S = \frac{aN_A S_0}{V_{std}} = \frac{V_L N_A S_0}{V_{std}} \quad (3)$$

From statistical thermodynamics, the relation between  $b$  in the Langmuir adsorption model and the temperature  $T$  can be expressed as follows (Gasser, 1987):

$$b(T) = b_0 e^{\frac{-\Delta H_{ad}}{RT}} / \sqrt{T} \quad (4)$$

and equation (4) can be rewritten as follows:

$$\ln(b\sqrt{T}) = \ln(b_0) - \frac{\Delta H_{ad}}{RT} \quad (5)$$

or

$$\ln\left(\sqrt{T} / P_L = \ln(b_0) - \frac{\Delta H_{ad}}{RT}\right) \quad (6)$$

According to equation (6), the relation between  $\ln(\sqrt{T} / P_L)$  and  $1/T$  is linear. The adsorption enthalpy  $\Delta H_{ad}$  and constant  $b_0$  can be obtained by fitting this formula to experimental data.

### 2.2.2 Theory of surface free energy

The change value of surface free energy refers to the change in this energy when CH<sub>4</sub> is adsorbed onto a unit area of the adsorbent for a constant temperature and pressure. Based on the principles of surface chemistry, the change value of coal surface free energy indicates the interaction capacity between the coal surface and CH<sub>4</sub>. The larger the change value of coal's surface free energy, the stronger the sorption capacity of the unit area (Zhang et al., 2011). According to surface chemistry theory, the change value of coal's surface free energy can be expressed as follows (Myers, 2002):

$$\Delta\sigma = -\int_0^P \sigma = \sigma_0 - \sigma = \int_0^P RT \frac{V}{V_{std}S} d \ln P \quad (7)$$

Substituting equations (2), (3) and (4) into equations (7) and (8) can be performed in the following form:

$$\Delta\sigma = \frac{RT}{V_{std}S} \int_0^P \frac{abP}{1+bP} d \ln P = \frac{RT}{N_A S_0} \ln \left[ 1 + (b_0 e^{\frac{\Delta H_{ad}}{RT}} / \sqrt{T}) P \right] \quad (8)$$

$R$ ,  $S_0$  and  $N_A$  are known quantities, and  $\Delta H_{ad}$  and  $b_0$  can be obtained by fitting equation (6) to experimental data. The change value of coal's surface free energy  $\Delta\sigma$  depends on the temperature  $T$  and pressure  $P$ .

### 2.3 Mass diffusivity method

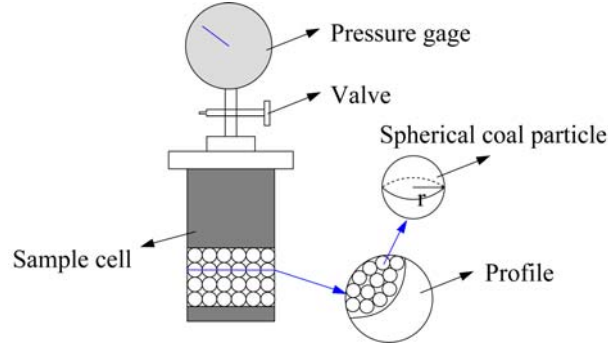
Research on the characteristics of gas diffusion, specifically, the mass diffusivity, can indicate the mass diffusivity of gas in a coal seam. The simplest method of determining the mass diffusivity to conduct diffusion experiments. The mass diffusivity can be determined by fitting the relevant formula to experimental data. In this paper, we choose the bulk technique for the desorption method to determine the diffusivity of CH<sub>4</sub> in coal. The coal samples in the sample cell are assumed to be spheroidal particles of the same radius. A portion of the desorption diffusion experimental device and a model of the coal particles are shown in Figure 2. Compared with the time required for gas diffusion in pores, the time required for gas flow in fractures is much shorter. In this paper, it is assumed that the gas desorption time is mainly affected by the diffusion effect; the time for gas flow in fractures is ignored (Jian et al., 2012).

The mechanisms of the gas diffusion process are very complex and are affected by many factors, but there is no doubt that pore size and pore structure are the main factors. The process of gas diffusion from macropores to micropores is controlled by many diffusion mechanisms. A detailed derivation of the mass diffusivity of a sphere with radius  $r$  is given by (Zhang, 2008) and relies on the following relation:

$$F = \frac{V_t}{V_0} = \frac{6}{\sqrt{\pi}} \frac{\sqrt{D}}{r} \sqrt{t} - \frac{D}{r^2} t \quad (9)$$



**Figure 2** Illustration for model of coal particles and parts of the experimental device (see online version for colours)



According to ref. (Jian et al., 2012), Jian has proved that the CO<sub>2</sub> mass diffusivity of coal is variable over time, and the same conclusion that the CH<sub>4</sub> mass diffusivity of coal is not constant is obtained using his approach. If  $D$  depends on time  $t$ , then the relation between  $F$  and  $t$  can be given as follows:

$$F = \frac{6}{\sqrt{\pi}} \frac{\sqrt{\int_0^t D dt'}}{r} \sqrt{t} - \frac{\int_0^t D dt'}{r^2} t \quad (10)$$

If we assume that  $x = \frac{\sqrt{\int_0^t D dt'}}{r}$ , equation (10) can be solved, and we obtain the following:

$$x = \frac{\sqrt{\int_0^t D dt'}}{r} = \frac{1}{\sqrt{\pi}} - \sqrt{\frac{1}{\pi} - \frac{F}{3}} \quad (11)$$

If we assume that  $y = \int_0^t D dt' = r^2 x^2$ , then

$$y = r^2 \left( \frac{1}{\sqrt{\pi}} - \sqrt{\frac{1}{\pi} - \frac{F}{3}} \right)^2 \quad (12)$$

The mass diffusivity  $D$  at a given time can be obtained as follows:

$$D = \frac{dy}{dt} \quad (13)$$

The relationship between  $t$  and  $F$  can be obtained using polynomial fitting. If the fitting formula and equation (12) are substituted into equation (13), then the  $D$  at a given time  $t$  can be determined.

### 3 Results

#### 3.1 Pore structures determined by mercury porosimetry and CO<sub>2</sub> adsorption

The intrusion and extrusion curves of the selected coal samples are shown in Figure 3, and the characteristics determined from mercury porosimetry are shown in Table 2.

**Figure 3** Intrusion and extrusion curves of selected coal samples (a) #1 and #2 coal samples (b) #3 and #4 coal samples (see online version for colours)

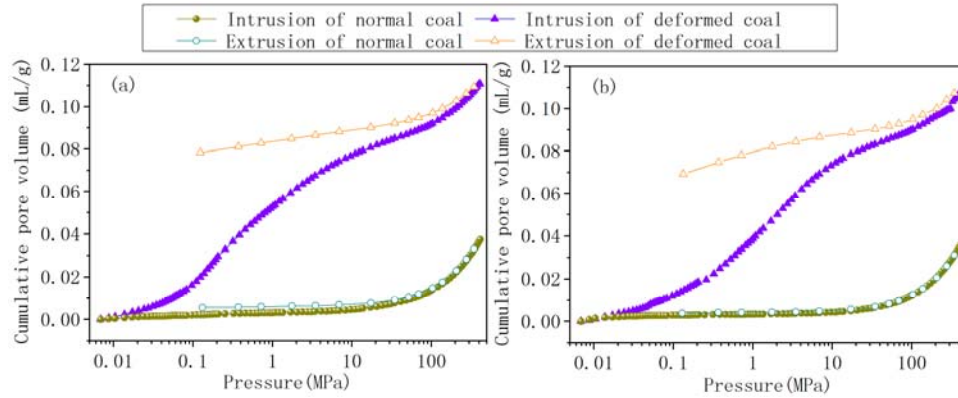


**Table 2** Characteristics of mercury porosimetry and CO<sub>2</sub> adsorption for selected coal samples

Sample no.	Mercury porosimetry					CO <sub>2</sub> adsorption	
	Total pore volume (mL/g)	Porosity (%)	Averaged PD (nm)	True density (g/mL)	Total SSA (m <sup>2</sup> /g)	D-A micropore volume (mL/g)	D-R micropore SSA (m <sup>2</sup> /g)
#1	0.1080	4.58	7.3	1.345	20.237	0.02022	57.98
#2	0.0357	13.32	485.3	1.423	17.179	0.01759	50.46
#3	0.1108	4.86	7.8	1.368	20.517	0.0215	61.67
#4	0.0374	13.82	1022.2	1.448	16.794	0.01594	45.71

Note: PD = pore diameter, SSA = specific surface area.

As Figure 3 shows, the cumulative mercury intrusion volume of deformed coal is much greater than that of normal coal at the same mercury pressure. The intrusion and extrusion curves of the two normal coal samples nearly overlap, and the hysteresis loop is not obvious. However, the intrusion and extrusion curves of the two deformed coal samples do not overlap, and the hysteresis loop is obvious. When the mercury pressure falls to 0 MPa, a considerable amount of mercury is still present in the deformed coal.

According to Table 2, the total pore volume and porosity of the deformed coal is 2.84 to 2.91 times greater than that of the normal coal, and the average pore diameter of the deformed coal is 66 to 132 times greater than that of the normal coal based on the mercury porosimetry. However, the total specific surface area of the normal coal is 1.18 to 1.22 times greater than that of the deformed coal. Tectonism destroys the original structure of the pores, which results in a greater total pore volume. When gas is adsorbed by coal, the skeleton of the coal softens. Moreover, compared with normal coal,

deformed coal has more pores of the same quality, which leads to thinner pore walls, making the coal much softer and more easily crushed. Although the pore system of deformed coal is well developed, its skeleton suffers more damage under situ stress conditions which reduces permeability, inhibits gas drainage and heightens the likelihood of coal and gas outbursts.

Coal micropores with diameters less than 2 nm play a major role in the total specific surface area and adsorption capacity of the coal (Clarkson and Bustin, 1999). Hence, in this study, the CO<sub>2</sub> adsorption method was used to evaluate the micropore characteristics of the selected coal samples. The DA equation is used to determine the micropore volume, and the DR equation is used to determine the specific surface area of the micropores. The results are shown in Table 2. Thus, the DA micropore volume and DR micropore-specific surface area of the normal coal are 1.15 to 1.35 times greater, respectively, than those of the deformed coal.

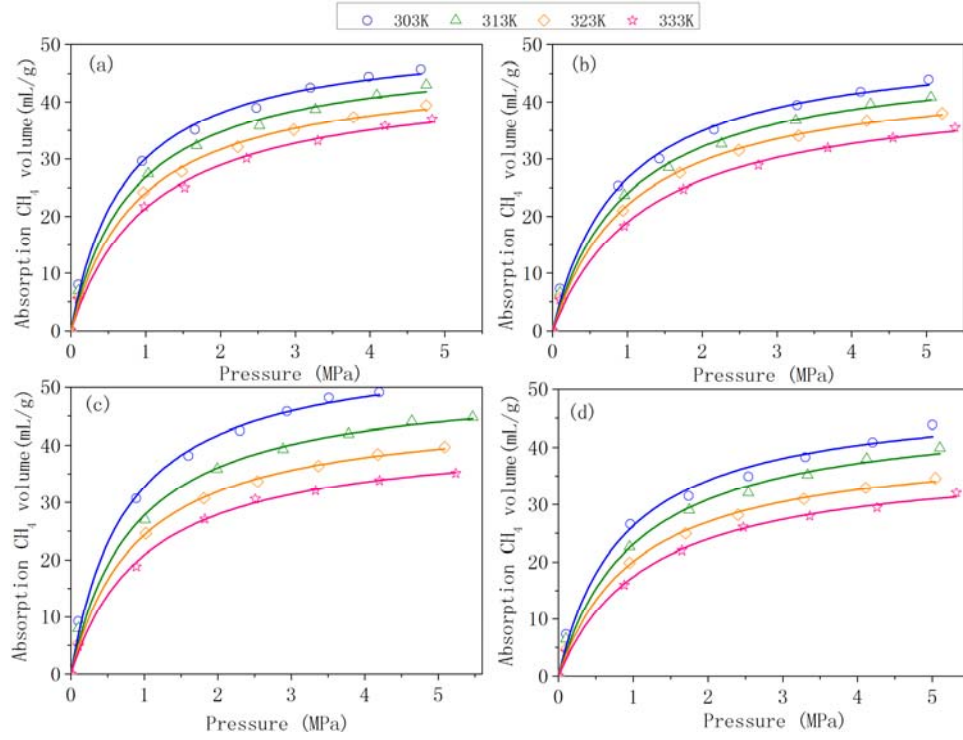
### 3.2 Adsorption capacity from CH<sub>4</sub> isotherms

Adsorption experiments were performed on normal coal and deformed coal at 303 K, 313 K, 323 K and 333 K. All CH<sub>4</sub> adsorption volumes at different temperatures were converted to volumes of standard condition. The adsorption isotherms of the coal samples at the different temperatures are shown in Figure 4. The Langmuir equation was used to fit the data, and the Langmuir volume and pressure results are collected in Table 3.

As Figure 4 shows, the CH<sub>4</sub> Langmuir volume ( $V_L$ ) of the normal coal and the deformed coal increase with increasing pressure but decrease with increasing temperature. At the same temperature and pressure, the CH<sub>4</sub> Langmuir volume ( $V_L$ ) of the normal coal is greater than that of the deformed coal. According to Table 4, the Langmuir volume ( $V_L$ ) of the normal coal and the deformed coal decrease with increasing temperature, but the Langmuir pressure ( $P_L$ ) of the normal coal and the deformed coal increase with increasing temperature. In addition, at the same temperature and pressure, the Langmuir pressure ( $P_L$ ) of the normal coal is lower than that of the deformed coal from the same location.

**Table 3** Langmuir volume ( $V_L$ ) and pressure ( $P_L$ ) of selected coal samples at different temperatures

Sample no.	Langmuir volume $V_L$ and pressure $P_L$	Temperature			
		303 K	313 K	323 K	333 K
#1	Langmuir volume $V_L$ (mL/g)	51.8892	49.1426	46.1807	44.5580
	Langmuir pressure $P_L$ (MPa)	0.7258	0.8324	0.9173	1.0814
#2	Langmuir volume $V_L$ (mL/g)	50.7703	48.5056	45.5454	43.0619
	Langmuir pressure $P_L$ (MPa)	0.9087	1.0219	1.0763	1.2719
#3	Langmuir volume $V_L$ (mL/g)	57.4795	51.4695	46.4196	42.1605
	Langmuir pressure $P_L$ (MPa)	0.7517	0.8525	0.9088	1.0233
#4	Langmuir volume $V_L$ (mL/g)	49.0714	46.7132	41.1608	38.4703
	Langmuir pressure $P_L$ (MPa)	0.8677	1.0247	1.0493	1.2091

**Figure 4** CH<sub>4</sub> adsorption isotherms of selected coal samples at different temperatures (a) #1 (b) #2 (c) #3 (d) #4 (see online version for colours)

At a temperature of 303 K, the Langmuir volume of #1 was 1.1189 mL/g greater than that of #2, and the Langmuir volume of #3 was 8.4081 mL/g more than that of #4. In addition, the Langmuir volume difference between #3 and #4 was greater than that between #1 and #2.

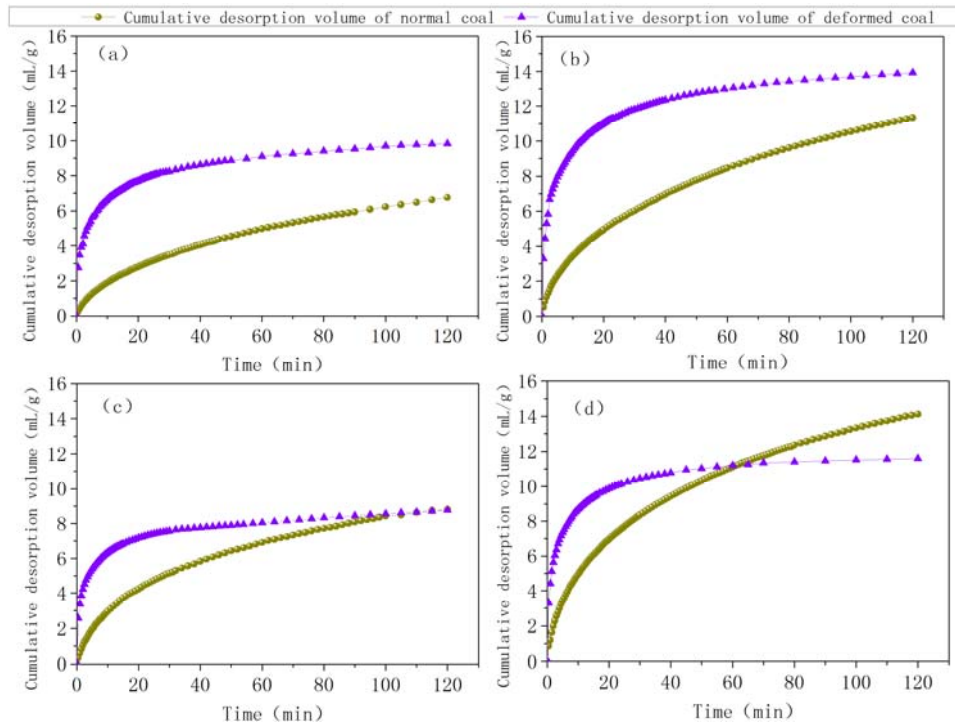
**Table 4** Relation between  $\ln(\sqrt{T}/P_L)$  and  $1/T$  obtained by fitting equation (6) and the  $\Delta H_{ad}$  and  $b_0$  values calculated from equation (4)

Sample no.	Relationship between $\ln(\sqrt{T}/P_L)$ and $1/T$	$\Delta H_{ad}/J/mol$	$b_0$
#1	$\ln(\sqrt{T}/P_L) = 1143.8 \times 1/T - 0.5926$	-9509.55	0.5529
#2	$\ln(\sqrt{T}/P_L) = 907.77 \times 1/T - 0.0374$	-7547.20	0.9633
#3	$\ln(\sqrt{T}/P_L) = 839.38 \times 1/T + 0.3673$	-6978.61	1.4438
#4	$\ln(\sqrt{T}/P_L) = 870.65 \times 1/T + 0.1093$	-7238.58	1.1155

### 3.3 $\text{CH}_4$ diffusion experiment

The initial pressures used in the desorption experiments were 0.8 MPa and 2.4 MPa. The relations between the cumulative desorption volume and desorption time for normal coal and deformed coal for the two different initial pressures at a temperature of 303 K are shown in Figure 5.

**Figure 5** Relations between cumulative desorption volume and desorption time of selected coal samples (a) #1 and #2 coal samples at 0.8 MPa (b) #1 and #2 coal samples at 2.4 MPa (c) #3 and #4 coal samples at 0.8 MPa (d) #3 and #4 coal samples at 2.4 MPa (see online version for colours)



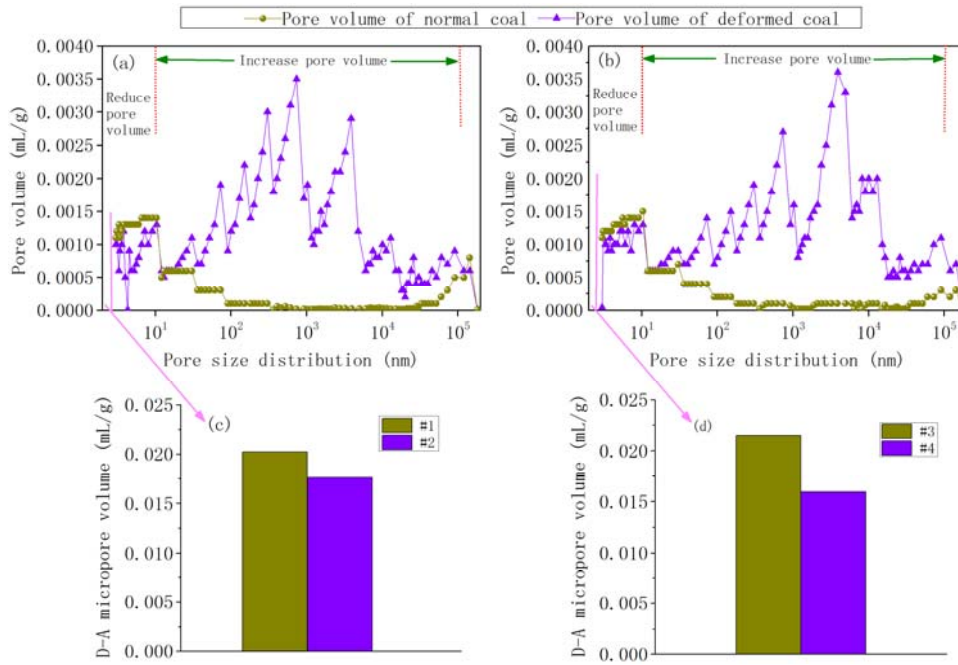
As Figure 5 shows, the cumulative desorption volumes of both the normal coal and the deformed coal increase steadily with time, which implies that the desorption speed of these two types of coal decreases with increasing desorption time. For the normal coal and deformed coal obtained from the same location, the initial desorption volume of the deformed coal is greater than that of the normal coal for the same initial pressure, which indicates that the initial desorption speed of the deformed coal is greater than that of the normal coal. Comparing the cumulative desorption volume of the normal coal and the deformed coal over a period of 120 min shows that the cumulative desorption volume of #2 is greater than that of #1 at one location. At the another location, however, the cumulative desorption volume of #3 overtakes that of #4 beginning at 100 min for an initial pressure of 0.8 MPa and at 60 min for an initial pressure of 2.4 MPa.

## 4 Discussion

### 4.1 Pore structure distributions

To assess the influence of tectonism on the coal's pore structure, the pore size distributions of the normal coal and the deformed coal determined from mercury porosimetry and the CO<sub>2</sub> adsorption results for symbiotic conditions are compared in Figure 6.

**Figure 6** Relations between pore size distribution and pore volume of selected coal samples (a) relations between pore size distribution and pore volume of #1 and #2 coal samples (b) relations between pore size distribution and pore volume of #3 and #4 coal samples (c) DA micropore volumes of #1 and #2 coal samples (d) DA micropore volumes of #3 and #4 coal samples (see online version for colours)



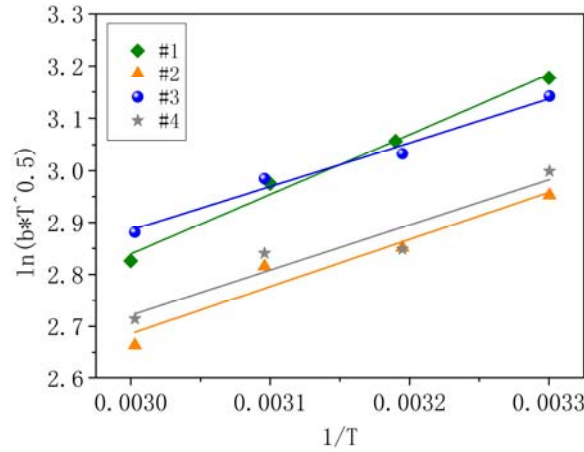
As Figure 6 shows, based on mercury porosimetry, the pores of the deformed coal with diameters between 10 and 10<sup>5</sup> nm are much larger than those of the normal coal; however, the pores in the 3–10 nm size range are slightly smaller than those of the normal coal. According to the CO<sub>2</sub> adsorption results, the DA micropore volume of the normal coal is also greater than that of the deformed coal, and the DA micropore volume difference between #3 and #4 is greater than that between #1 and #2. The stress and temperature effects of tectonism play a primordial role in the development of coal (Ju and Li, 2009). Physical destruction from stress is the reason that deformed coal has more pores within the 10–10<sup>5</sup> nm size range than normal coal. Tectonism can cause the parameters of deformed coal to have a much higher-rank of coal than that at the side of normal coal. The  $R_{o, \max}$  of the deformed coal is higher than that of the normal coal, as

shown in Table 1. The pores in the 3–10 nm size range and the DA micropores in the deformed coal are deformations of the macromolecular structure caused by the stress and temperature effects of tectonism. These effects may also lead to changes in the nanoscale pore structure ( $d < 100$  nm) (Ju and Li, 2009).

#### 4.2 The change value of coal surface free energy

According to equation (6), the relation between  $\ln(\sqrt{T}/P_L)$  and  $1/T$  is linear, as shown in Figure 7. The adsorption enthalpy  $\Delta H_{ad}$  and constant  $b_0$  can be determined by fitting the formula to the experimental data. The values of  $H_{ad}$  and  $b_0$  are shown in Table 4.

**Figure 7** Relation between  $\ln(b\sqrt{T})$  and  $1/T$  of selected coal samples (see online version for colours)

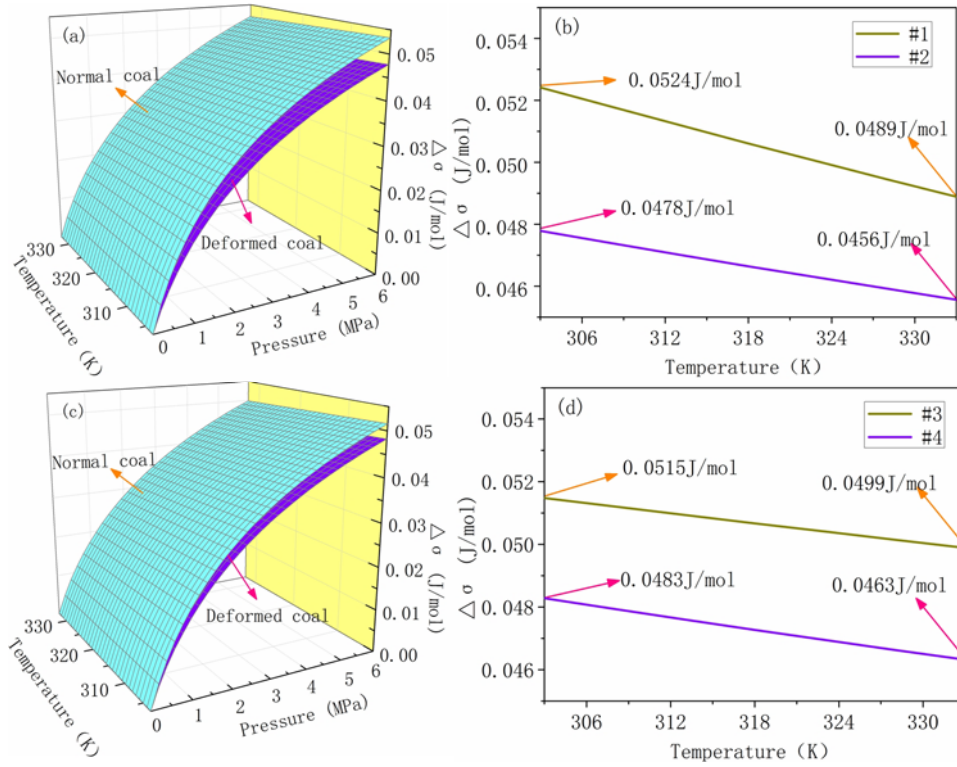


Based on the results shown in Table 5, the fitting formula and corresponding parameters are entered into equation (8). The change values of the coal surface free energy  $\Delta\sigma$  of the selected coal samples change with pressure and temperature, as shown in Figure 8.

Coal is an amorphous, three-dimensional, and highly crosslinked polymer. The core structural unit of coal consists of an aromatic nucleus connected to alicyclics, side chains and functional groups by various bridge bondings. Hence, coal can be seen as an organic combination of carbon atoms. In coal, due to the force effects of adjacent carbon atoms, internal carbon atoms are attracted to each other in the stress equilibrium state. However, the surface carbon atoms on at least one side are empty, resulting in a state of stress disequilibrium, which leads to surface carbon atoms tending to move toward the interior of the coal body. This tendency gives surface carbon atoms extra energy, which is called the surface free energy. According to the lowest energy principle, any interface spontaneously reduces the trend of interfacial energy, but the solid surface atoms cannot easily move to reduce their surface energy. The only way that they can do so is through the adsorption of other gas molecules, which is the fundamental driving force that causes coal adsorption.



**Figure 8**  $\Delta\sigma$  changes with pressure and temperature for selected coal samples (a)  $\Delta\sigma$  changes with pressure and temperature for #1 and #2 coal samples (b)  $\Delta\sigma$  changes with pressure and temperature for #3 and #4 coal samples (c)  $\Delta\sigma$  changes with temperature for #1 and #2 DEF coal samples at 6 MPa (d)  $\Delta\sigma$  changes with temperature for #3 and #4 coal samples at 6 MPa (see online version for colours)



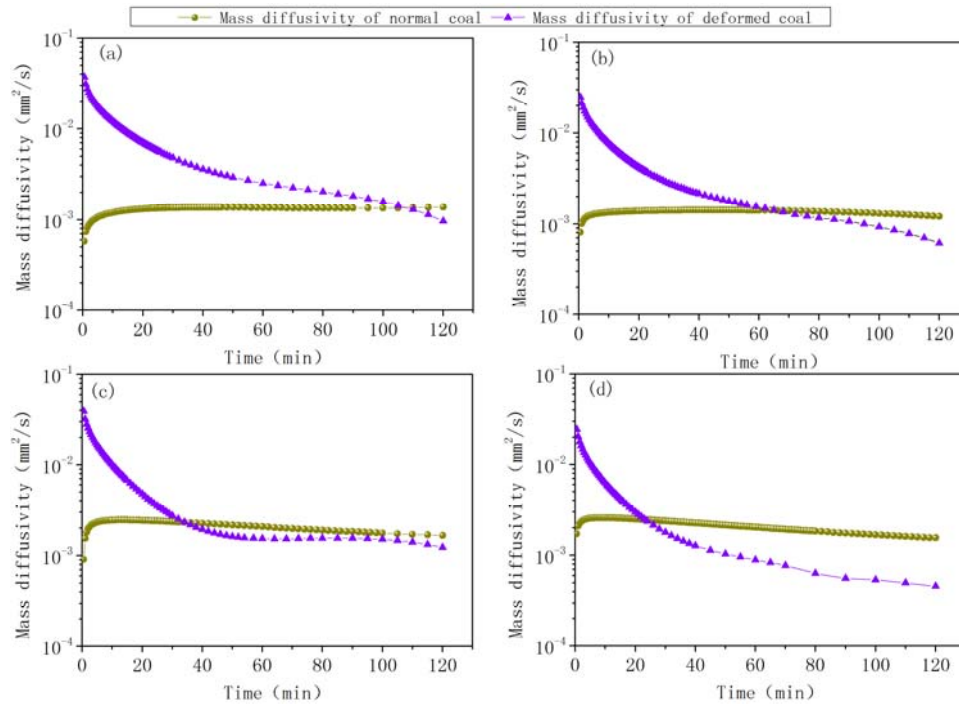
The larger the change value of the coal surface free energy, the stronger the sorption capacity per unit area will be. As Figure 8 shows, at a certain temperature, the  $\Delta\sigma$  of the normal coal and the deformed coal increases with increasing pressure, which indicates that increasing pressure causes the coal surface to adsorb more  $\text{CH}_4$  gas and makes the coal surface free energy tend toward a low-energy state. At a pressure of 6 MPa, the  $\Delta\sigma$  of the normal coal and the deformed coal decrease with increasing temperature, which can increase the activity of methane molecules and make them difficult to capture. The  $\Delta\sigma$  of normal coal is greater than that of deformed coal under symbiotic conditions, which indicates that the  $\text{CH}_4$  adsorption capacity of normal coal is higher than that of deformed coal. The pore measurement results indicate that the total specific surface area of the micropores within the size range of 3–10 nm and the micropores ( $d < 2$  nm) in the normal coal are larger than those of the micropores of the same size in the deformed coal. Moreover, in the high-pressure adsorption stage, the skeleton of the deformed coal starts to deform more easily. This is called the pore compression effect, and it reduces the porosity and forms new bottlenecks that reduce the  $\text{CH}_4$  adsorption capacity of deformed coal.



### 4.3 Mass diffusivity

The relationship between  $t$  and  $F$  can be determined using polynomial fitting. The fitting formula and equation (12) are substituted into equation (13); and  $D$  at a given time  $t$  can be determined. The relationship between the calculated CH<sub>4</sub> mass diffusivity and time at a temperature of 303 K is shown in Figure 9.

**Figure 9** Relations between mass diffusivity and time for selected coal samples (a) #1 and #2 coal samples at 0.8 MPa (b) #1 and #2 coal samples at 2.4 MPa (c) #3 and #4 coal samples at 0.8 MPa (d) #3 and #4 coal samples at 2.4 MPa (see online version for colours)



In the early stages of the coal desorption process, the mass diffusivity of deformed coal is approximately 10 times greater than that of normal coal. The mass diffusivity of deformed coal decreases rapidly, while that of normal coal decreases very slowly. After a certain period of time (from 20 to 100 minutes) which depends on the coal sample characteristics and the initial desorption pressure, the mass diffusivity of deformed coal will be less than that of normal coal. This occurs for several reasons.

- 1 The analysed coal particles are assumed to be spheres in the desorption process. Initially, the desorbed gas from the particle surfaces and macropores can easily reach the coal particle surfaces. With the passage of time, the desorbed gas from the particles needs to overcome the pore network resistance to reach the coal particle surfaces, which will cause both the mass diffusivity of normal coal and that of deformed coal to decrease gradually with time. Initial desorption is strongly influenced by macropores from which gas rapidly escapes (Crosdale et al., 1998). As the mercury porosimetry shows, the deformed coal has more pores within the size

range of 10 to  $10^5$  nm than the normal coal, so the initial mass diffusivity of the deformed coal is much larger than that of the normal coal. However, longer-term desorption is controlled by the micropores. The  $\text{CO}_2$  adsorption shows that the deformed coal pores within the size range of 3–10 nm pores and the DA micropores are slightly smaller than those in normal coal, after a period of time, the mass diffusivity of deformed coal will be slightly smaller than that of normal coal.

- 2 The shrinkage of coal matrices during desorption can increase volumetric strain and reduce the pore size (Harpalani and Chen, 1995; Harpalani and Chen, 1997) and can make it more difficult for gas to be diffused out of the coal particles, leading to a higher mass diffusivity. The mass diffusivity of deformed coal changes with time becoming more than that of normal coal, because the wall skeleton of deformed coal is more easily affected by the shrinkage of coal matrices than normal coal. For the reasons stated above, the mass diffusivity of coal is concluded to be governed by the mechanisms of the gas diffusion process, due to the differences between normal coal and deformed coal in terms of original pore size distribution, as well as the effects of matrix volume strain. As the desorption process changes from macropore diffusion at early stages to micropore diffusion at later stages, the main mechanisms of the gas diffusion process change from pore diffusion and transition diffusion to Knudsen diffusion and surface diffusion.

The changes in the mass diffusivity of the two deformed coal samples with time were much more obvious than those of the two normal coal samples. The ranges of variational diffusivity values of the two normal coal samples were  $0.578 \times 10^{-3}$  to  $1.434 \times 10^{-3} \text{ mm}^2/\text{s}$  and  $0.809 \times 10^{-3}$  to  $2.466 \times 10^{-3} \text{ mm}^2/\text{s}$  and those of the two deformed coal samples were  $0.618 \times 10^{-3}$  to  $3.712 \times 10^{-2} \text{ mm}^2/\text{s}$  and  $0.464 \times 10^{-3}$  to  $3.897 \times 10^{-2} \text{ mm}^2/\text{s}$ . The maximum mass diffusivity of the normal coal was found to be three times greater than its minimum mass diffusivity, while the maximum mass diffusivity of the deformed coal was found to be 100 times greater than its minimum mass diffusivity. These results are consistent with results obtained by other researchers (Clarkson and Bustin, 1999). The reason for the difference between the maximum and minimum mass diffusivity of the two types of coal is that the desorption process changes from macropore diffusion in the early stages to micropore diffusion at later stages (Ruckenstein et al., 1971).

## 5 Conclusions

- 1 Mercury porosimetry tests showed that the total pore volume and porosity of deformed coal is 2.84 to 2.91 times greater than that of normal coal.  $\text{CO}_2$  adsorption tests showed that the DA micropore volume and DR micropore specific surface area of normal coal are respectively 1.15 to 1.35 times greater than those of deformed coal. Tectonism increases the number of 10 to  $10^5$  nm pores and reduces the number of 3 to 10 nm pores and DA micropores ( $d < 2$  nm).

- 2 For a given temperature and pressure, the Langmuir volume ( $V_L$ ) of the normal coal is greater than that of the deformed coal, but the Langmuir pressure ( $P_L$ ) of the normal coal is lower than that of the deformed coal from the same location. The larger sorption capacity of deformed coal is partially due to its greater micropore specific surface area. The  $\Delta\sigma$  of normal coal is slightly greater than that of deformed coal, which indicates that the unit area of normal coal CH<sub>4</sub> adsorption capacity is also greater than that of deformed coal. More pores of the same quality exist in deformed coal, which results in thinner pore walls that are much more easily crushed. In the high-pressure adsorption stage, the pore compression effect reduces the CH<sub>4</sub> adsorption capacity of deformed coal.
- 3 In the early stages of the coal desorption process, the initial desorption volume of deformed coal is greater than that of normal coal, and the mass diffusivity of deformed coal is approximately ten times greater than that of normal coal. The mass diffusivity of deformed coal decreases rapidly, while that of normal coal decreases very slowly. After a certain period of time (from 20 to 100 minutes) which depends on the coal sample characteristics and the initial desorption pressure, the mass diffusivity of deformed coal will be less than that of normal coal.

Deformed coal has more pores of the same quality, which leads to thinner pore walls and more free methane in deformed coal. However, the skeleton of deformed coal is more damaged in situ stress conditions that reduce the permeability, which can block methane migration, inhibit gas drainage and result in pocket of high methane pressure. What's more, the initial larger mass diffusivity and desorption volume of deformed coal will heighten the likelihood of coal and gas outbursts. A certain thickness of deformed coal plays a key role in coal and gas outbursts, but understanding of the microscopic characteristics of deformed coal is still very limited. Considering the lower because of more pores and the initial larger mass diffusivity and desorption volume of deformed coal, the firmness coefficient and initial desorption volume of deformed coal should be better used in prevention coal and gas outbursts, and pressure relief antireflective and hydraulic fracturing technologies can heighten the permeability of deformed coal, more bores and increasing the rate of bore forming technology should be applied in gas drainage in deformed coal.

### Acknowledgements

The authors would like to thank Editor Prof. Shaoxian Song and M.R. Riazi at the IJOGCT and reviewers of this paper for their critical and constructive review of this paper. Financial support provided by the National Basic Research Program of China (973 Program, No. 2011CB201204), the National Foundation of China (No. 51074160), the Natural Science Foundation for the Youth of China (No. 41202118 and No. 51204173).

### Notation

$d_i$	Pore diameter of mercury intrusion pressure, $\mu\text{m}$ ; $p_i$ Mercury intrusion pressure, psia
$\gamma$	Surface tension of mercury, N/m; $\theta$ Contact angle of mercury, $130^\circ$
$V$	Gas adsorption volume of unit mass adsorbent, mL/g; $V_L$ Langmuir volume, $V_L = a$ , mL/g
$P_L$	Langmuir pressure, $P_L = 1/b$ , MPa; $P$ Pressure, MPa
$N_A$	Avogadro number, $6.023 \times 10^{23}$ ; $S$ Adsorbent specific surface area of unit mass, $\text{m}^2/\text{g}$
$S_0$	$\text{CH}_4$ molecular sectional area, $1.78 \times 10^{-19} \text{ m}^2$ ; $V_{std}$ Standard state gas molar volume, $22.4 \times 10^3 \text{ mL/g}$
$\Delta H_{ad}$	Adsorption enthalpy, J/mol; $b_0$ Constant related to adsorption molecular
$R$	Gas constant, J/(mol $\times$ K); $T$ Temperature, K
$\Delta\sigma$	Change value of surface free energy, J/mol; $\sigma_0$ Initial surface free energy, J/mol
$\Sigma$	Adsorbed surface free energy, J/mol; $D$ Mass diffusivity, $\text{mm}^2/\text{s}$
$t$	Time, min; $r$ Average radius of coal particles, 2 mm
$F$	$\text{CH}_4$ desorption volume percent; $V_0$ $\text{CH}_4$ desorption maximum volume, mL/g
$V_t$	$\text{CH}_4$ desorption volume within a time, mL/g

### References

- Amarasekera, G., Scarlett, M.J. and Mainwaring, D.E. (1975) 'Micropore size distributions and specific interactions in coals', *Fuel*, Vol. 74, No. 1, pp.115–118.
- ASTM (2007) 'Annual Book of ASTM Standards', *Section Five, Petroleum Products, Lubricants, and Fossil Fuels*, Vol. 05.06, ASTM International, West Conshohocken, PA.
- BS ISO 15901-1 (2005) *Pore Size Distribution and Porosity of Solid Materials by Mercury Porosimetry and Gas Adsorption: Mercury Porosimetry*, British Standards Institution, London.
- BS ISO 15901-3 (2007) *Pore Size Distribution and Porosity of Solid Materials by Mercury Porosimetry and Gas Adsorption. Analysis of Micropores by Gas Adsorption*, British Standards Institution, London.
- BS ISO 7404-5 (2009) *Methods for the Petrographic Analysis of coals. Method of Determining Microscopically the Reflectance of Vitrinite*, British Standards Institution, London.
- Busch, A., Gensterblum, Y., Krooss, B.M. and Littke, R. (2004) 'Methane and carbon dioxide adsorption/diffusion experiments on coal: upscaling and modeling approach', *International Journal of Coal Geology*, Vol. 60, Nos. 2–4, pp.151–168.
- Cao, Y.X., Davis, A., Liu, R.X., Liu, X.W. and Zhang, Y.G. (2003) 'The influence of tectonic deformation on some geochemical properties of coals – a possible indicator of outburst potential', *International Journal of Coal Geology*, Vol. 53, No. 2, pp.69–79.
- Cattaneo, C., Manera, M. and Scarpa, E. (2011) 'Industrial coal demand in China: a provincial analysis', *Resource and Energy Economics*, Vol. 33, No. 1, pp.12–35.
- Clarkson, C.R. and Bustin, R.M. (1999) 'The effect of pore structure and gas pressure upon the transport properties of coal: a laboratory and modeling study. 2. Adsorption rate modeling', *Fuel*, Vol. 78, No. 11, pp.1345–1362.

- Clarkson, C.R., Bustina, R.M. and Levy, J.H. (1997) 'Adsorption potential theories to coal methane adsorption isotherms at elevated temperature and pressure', *Carbon*, Vol. 35, No. 12, pp.1689–1705.
- Crosdale, P.J., Beamish, B.B. and Valix, M. (1998) 'Coalbed methane sorption related to coal composition', *International Journal of Coal Geology*, Vol. 35, Nos. 1–4, pp.147–158.
- Gasser, R.P.H. (1987) *An Introduction to Chemisorption and Catalysis by Metals*, pp.1–13, Oxford Science Publishers, Clarendon Press, Oxford.
- Harpalani, S. and Chen, G.L. (1995) 'Estimation of changes in fracture porosity of coal with gas emission', *Fuel*, Vol. 74, No. 10, pp.1491–1498.
- Harpalani, S. and Chen, G. (1997) 'Influence of gas production induced volumetric strain on permeability of coal', *Geotechnical and Geological Engineering*, Vol. 15, No. 4, pp.303–325.
- Hower, J.C. (1997) 'Observation on the role of Bernice coal field (Sullivan County, Pennsylvania) anthracites in the development of coalification theories in the Appalachians', *International Journal of Coal Geology*, Vol. 33, No. 2, pp.95–102.
- Jian, X., Guan, P. and Zhang, W. (2012) 'Carbon dioxide sorption and diffusion in coals: Experimental investigation and modeling', *Science China: Earth Sciences*, Vol. 55, No. 4, pp.633–643.
- Jiang, B., Qu, Z.H., Wang, G.G.X. and Li, M. (2010) 'Effects of structural deformation on formation of coalbed methane reservoirs in Huaibei coalfield, China', *International Journal of Coal Geology*, Vol. 82, Nos. 3–4, pp.175–183.
- Ju, Y.W. and Li, X.S. (2009) 'New research progress on the ultrastructure of tectonically deformed coals', *Progress in Natural Science*, Vol. 19, No. 11, pp.1455–1466.
- Langmuir, I. (1918) 'The adsorption of gases on plane surfaces of glass, mica and platinum', *J. Am. Chem. Soc.*, Vol. 40, No. 9, pp.1361–1403.
- Li, H.Y. (2001) 'Major and minor structural features of a bedding shear zone along a coal seam and related gas outburst, Pingdingshan coalfield, northern China', *International Journal of Coal Geology*, Vol. 47, No. 2, pp.101–113.
- Li, M., Jiang, B., Lin, S.F., Wang, J.L., Ji, M.J. and Qu, Z.H. (2011) 'Tectonically deformed coal types and pore structures in Puhe and Shanchahe coal mines in western Guizhou', *Mining Science and Technology*, Vol. 21, No. 3, pp.353–357.
- Myers, A.L. (2002) 'Thermodynamics of adsorption in porous materials', *AIChE*, Vol. 48, No. 1, pp.145–159.
- Ruckenstein, E., Vaidyanathan, A.S. and Youngquist, G.R. (1971) 'Sorption by solids with bidisperse pore structures', *Chemical Engineering Science*, Vol. 26, No. 9, pp.1305–1318.
- Taylor, G.H., Teichmüller, M., Davis, A., Diessel, C.F.K., Littke, R. and Robert, P. (1998) *Organic Petrology*, Gebrüder Borntraeger, Berlin.
- Wang, Y.A. and Yang, S.M. (1980) 'Some characteristics of coal seams with hazard of outburst', *Journal of China Coal Society*, Vol. 5, No. 1, pp.47–53 (in Chinese with an English abstract).
- Wen, Z.H., Wei, J.P., Wang, D.K. and Wang, C. (2011) 'Experimental study of gas desorption law of deformed coal', in He, X et al (Ed.): *First International Symposium on Mine Safety Science and Engineering*, Vol. 26, pp.1083–1088, Beijing, China.
- Yang, H.M., Huo, X.Y. and Zhang, S.J. (2012a) 'Study on difference of outburst elimination effect between sub-layers of soft coal and hard coal under the condition of gas per-drainage', *Safety Science*, Vol. 50, No. 4, pp.768–772.
- Yang, W., Lin, B.Q., Zhai, C., Li, X.Z. and An, S. (2012b) 'How in situ stresses and the driving cycle footage affect the gas outburst risk of driving coal mine roadway', *Tunnelling and Underground Space Technology*, Vol. 31, No. 9, pp.139–148.
- Yao, D.X. and Lv, J. (1996) 'Pore characteristics of coal in Xieyi coal mine in Huainan coalfield', *Coal Geology of China*, Vol. 8, No. 4, pp.31–33 (in Chinese).

- Zhang, L., Aziz, N., Ren, T.X. and Wang, Z.W. (2011) 'Influence of temperature on coal sorption characteristics and the theory of coal surface free energy', in He, X et al (Ed.): *First International Symposium on Mine Safety Science and Engineering, Procedia Engineering*, Vol. 26, 1430–1439, Beijing, China.
- Zhang, Y.X. (2008) *Geochemical Kinetics*, pp.224–227, 284–298, 418–434, Princeton University Press, Boston.
- Zhang, Z.G. (2011) 'Research on gas irradiation feature of tectonic coal', in He, X et al. (Ed.): *First International Symposium on Mine Safety Science and Engineering*, Vol. 26, pp.154–159, Beijing, China.